SENTINEL-2 RADIOMETRIC UNCERTAINTY TOOL

Javier Gorroño [(1)], Ferran Gascon [(2)]

[(1)] National Physical Laboratory, Hampton Road, Teddington, Middlesex, TW11 0LW (UK), Email: javier.gorrono@npl.co.uk
[(2)] European Space Agency, ESA/ESRIN, Via Galileo Galilei, Casella Postale 64, 00044 Frascati (Roma, Italy), Email:ferran.gascon@esa.int

ABSTRACT

In the framework of the European Copernicus programme, the European Space Agency (ESA) will launch the Sentinel-2 (S2) Earth Observation (EO) mission which will provide optical high spatial resolution imagery over land and coastal areas. In order to exploit Sentinel-2 imagery, several applications require having an uncertainty value associated to the measurements. This paper presents a tool (named S2-RUT, from Sentinel-2 Radiometric Uncertainty Tool) allowing estimating the radiometric uncertainties associated to each pixel using as input the top-of-atmosphere (TOA) reflectance images provided by ESA. The tool is based on a radiometric model of the S2 measurements, covering both the satellite sensor and the ground processing. The uncertainty of each model parameter is characterised and uncertainties propagated through the radiometric model. The methodology used follows the guidelines proposed by the Quality Assurance Framework for Earth Observation (QA4EO) and aims to provide a transparent and traceable radiometric uncertainty analysis for users of S2 data.

1. INTRODUCTION

The Copernicus programme is an EU-led initiative. It consists of a complex set of systems which collect data from multiple sources (earth observation satellites and *in situ* sensors) as well as the processing of these data and its distribution to the users. This data is divided in six thematic areas: marine, land, atmosphere, emergency, security and climate change [1]. The European Space Agency (ESA) is responsible for the Copernicus space component. This is comprised of two types of satellite missions, ESA's five families of dedicated Sentinels and missions from other space agencies; known as 'Contributing Missions'. A unified ground segment, through which data is streamed and made freely available for Copernicus services, completes the Space Component [2].

S2 is one of the Sentinel missions mainly devoted to Land Monitoring, Emergency Response, and Security Copernicus services. The S2 mission will provide high-resolution optical observations over global terrestrial surfaces and some of the specific applications will contribute, for instance, to urban planning, natural and man-made disasters management or crop monitoring. S2 will have a set of unprecedented capabilities with respect to other multi-spectral missions. Specifically, the S2 mission will provide 13 VNIR bands with spatial resolutions of 10 m, 20 m and 60 m as well as a short revisit time (5 days at the equator) and a wide field of view (290 km) [3], [4].

A radiometric uncertainty analysis tool (S2-RUT) has been developed. This tool follows the established procedures described in the QA4EO guidelines and/or the Guide to the Expression of Uncertainty in Measurement (GUM) [5]. The S2-RUT allows calculating the absolute radiometric uncertainty for each pixel from the S2 Level-1C products (TOA reflectance/radiance images).

In this paper, we describe the design and implementation of the S2-RUT tool as well as the uncertainty analysis performed. Section II describes the basic features of the S2 mission and the Multi Spectral Instrument (MSI). Section III details the S2 uncertainties analysis performed. The MSI radiometric model is first described and then decomposed into different uncertainty contributors which are explained individually in order to propose a combination.

In Section IV the tool design and the implementation of the S2-RUT is explained.

2. MSI INSTRUMENT AND MISSION OVERVIEW

The S2 mission is an optical high spatial resolution mission for Copernicus operational services. with a systematic global coverage of all land surfaces from 56° South to 84° North;a high revisit frequency: (5 days at equator); high spatial resolution: (10 m, 20 m and 60 m depending on the bands); 13 bands covering the spectral range from visible to short wave infra-red and a wide field of view of 290 km [4].

Proc. 'ESA Living Planet Symposium 2013', Edinburgh, UK
9–13 September 2013 (ESA SP-722, December 2013)

This will be possible thanks to a polar orbiting satellite constellation of two units carrying each one the MSI instrument. It consists of a push-broom scanning with monolithic complementary metal oxide semiconductor (CMOS) detectors for the VNIR focal plane, while the SWIR focal plane is based on mercury−cadmium−telluride (MCT) detectors hybridised on a CMOS readout circuit. It includes twelve VNIR and SWIR detectors employed in a staggered configuration separating spectrally the VNIR and SWIR channels by a dichroic beam splitter. The radiometric calibration is based in a full-field and full-pupil on-board diffuser. The observation data will be digitised using 12 bits and sent to the ground stations using a state-of-the-art lossy compression [4].

3. UNCERTAINTY ANALYSIS

The S2-RUT associates a QI (in this case radiometric uncertainty) to the S2 Level-1C product by generating a Level-1C radiometric uncertainty image. This uncertainty analysis has been based in the guidelines provided by the GUM and the QA4EO guidelines for uncertainty measurements [5] [7].

This chapter gives the detail of the radiometric S2 radiometric uncertainty analysis performed. Firstly in **section A**, the model that describes the S2 radiometry is presented. From each of the parameters, different uncertainty contributions can be characterised and measured; these are explained sequentially in **sections B, C, D and E**. Finally, **section F** proposes a combination for the uncertainty contributions.

3.1. Model

The first step of the analysis is the setup of a radiometric model. The schematic in Fig.1a and Fig.1b decompose the radiometric satellite acquisition and the ground processing chain model respectively.

In Fig.1a the ***Earth radiance*** is collected by the MSI instrument and translated into digital counts or **raw signal (***X*). The signal (*X*) is compressed and equalised on-board by the **Video Compression Unit (VCU)** and sent to the ground stations (*Z'vcu*). The next steps are considered as part of the Level-1 on-ground processing (Fig.1b): 1) decompression of the signal and inversion of the equalisation in order to recover the signal (*X*) at **VCU^{-1}**, 2) **Dark Signal (** $DS(p,l \bmod i,d)$ **)** and the **pixel contextual offset (** $PC_{masked}(l,b,d)$ **)** removal obtains the **dark signal corrected output (***Y(p,l,b,d)*), 3) application of the **gamma function** $\gamma(p,b,d,Y)$ to compensate for the non-linear response of each pixel and to obtain $Z(p,l,b,d)$, 4) **deconvolution and signal denoising,** 5) translation into **top-of-atmosphere radiances (** $R_{eq}(p)$ **)** by the **Absolute Coefficients (***A(b)*) and 6) resampling in order to obtain the **L1C product reflectance (** $R_{L1c}(p)$ **)**.The parameter *p* refers to the considered pixel, *l* refers to the considered line, *b* refers to the specific spectral channel, *d* refers to the specific detector and *i* depends on the number of lines averaged for the calculation of DS (over the lines modulo 6 for 10m bands, modulo 3 for 20m bands and over all lines for 60m bands).

In equations (1a), (1b), (1c) and (1d) the different processes in Fig.1a and Fig.1b are all linked by means of a mathematical model:

$$R_{L1c}(p) = f_{resampling}(p,b,d,R_{eq}(p)) \quad (1a)$$

$$R_{eq}(p) = \frac{Z(p,l,b,d) + \text{denoising}_{residual}}{A(b)} \quad (1b)$$

$$Z(p,l,b,d) = \gamma(p,b,d,Y) \quad (1c)$$

$$Y(p,l,b,d) = X(p,l,b,d) - DS(p,l \bmod i,d) - PC_{masked}(l,b,d) \quad (1d)$$

where:

- $f_{resampling}$ represents the resampling function (cubic spline)
- $\text{denoising}_{residual}$ refers to the correction residual as a result of the denoising correction

In turn, each one of the processes can be modelled and decomposed into several contributors as in equations (3), (4) and (5a).

The effect of this compression (VCU^{-1}) has been studied by the instrument prime-contractor concluding that the effect is negligible. However, during the commissioning phase these levels could be changed and, therefore, its impact on the radiometric performance could change as well.

The uncertainty introduced by the denoising residual, and that introduced as a consequence of the resampling function have not been analysed in a great amount of detail. However, both processing steps have been highlighted as potential sources of uncertainty that would need to be further investigated.

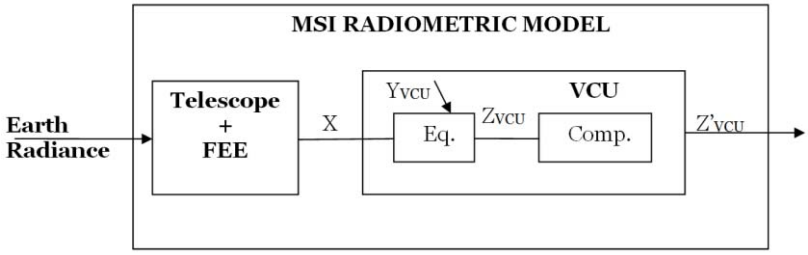

Figure1a. Flow diagram showing the S2 radiometric acquisition (satellite payload) model.

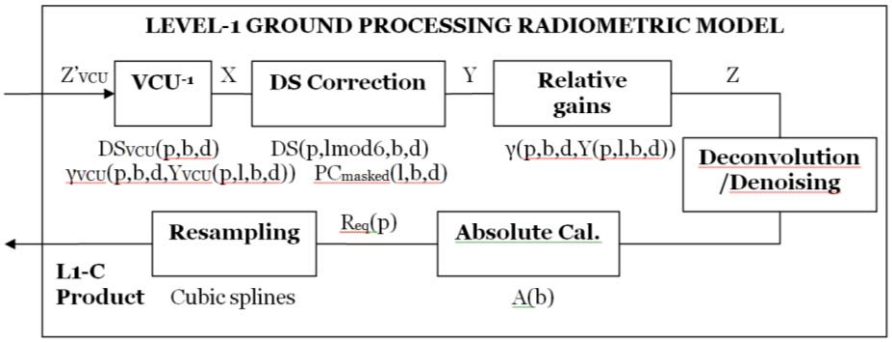

Figure1b Flow diagram showing the S2 radiometric ground processing chain

3.2. Uncertainty Contributors: X(p,l,b,d)

The raw signal (referred as $X(p,l,b,d)$) is the data received on-ground after decompression in nominal mode. The main sources are:

- *Optical crosstalk*: mainly produced between the filter assembly and the detectors where multiple reflexion/diffusion can occur. The uncertainty levels have been based on predicted levels.
- *Electrical crosstalk*: refers to the interference between signals transferring through the hardware in the detection chain. The contributing components are the detector crosstalk, the VCU and the Front-End Electronics (FEE). Their individual effects have been quadratically summed to obtain the overall electrical crosstalk.
- *Straylight*: refers to light reaching the satellite sensor through an alternative path or from another source rather than the Earth (e.g. sun). This light will be translated into a bias of 0.3% in L_{ref} for VNIR channels and 0.15% for SWIR channels (where L_{ref} refers to the reference radiance level).
- *MSI noise:* noise is the combination of the dark noise, readout noise, electronic noise and shot noise. As the combined noise is proportional to the input signal, the uncertainty for this contributor has been provided as a percentage of the incoming radiance. The noise measurements were calculated at L_{ref} .However, these noise values have been extrapolated to L_{max} and L_{min} (where L_{max} and L_{min} represents the predefined maximum and minimum radiances of the S2 radiance range) using the noise model in (2):

$$Noise\_Z(p,l,b,d) = \sqrt{(\alpha\_Z(p,b,d))^2 + \beta\_Z(p,b,d)\cdot Z(p,l,b,d)} \quad (2)$$

$$\alpha\_Z(p,b,d) = STD_l\left[Z_{ds}(p,l,b,d)\right]$$

$$\beta\_Z(p,b,d) = \frac{STD_l^2\left[Z_{sd}(p,l,b,d)\right] - (\alpha\_Z(p,b,d))^2}{A(b)\cdot K_{slt}\cdot\frac{1}{N_l}\cdot\sum_l \frac{\rho(p,\theta_{sd}(l),\varphi_{sd}(l))}{\pi}\cdot\frac{E_{sun}(b)}{d_{sun}^2}\cdot\cos\theta_{sd}(l)}$$

where $Z_{ds}(p,l,b,d)$ is the signal obtained by measuring the DS, $Z_{sd}(p,l,b,d)$ is the signal obtained in calibration mode, and α_Z and β_Z are dimensionless noise model. .

In the equation for β_Z, the term $\rho(p,\theta_{sd}(l),\phi_{sd}(l))$ refers to the reflectance produced by the sun-diffuser. The term $E_{sun}(b)$ refers to the sun irradiance value for each band obtained from Thuillier solar irradiance model [8].

The term $\cos\theta_{sd}(l)$ refers to the cosine dependence of the diffuser. The term d_{sun} refers to the satellite-to-sun distance. The straylight during calibration is represented by the correction factor K_{slt}. The term N_l is the number of lines.

- *Polarisation:* the MSI instrument has been designed to reduce the effects of polarisation. Nevertheless, the uncertainty produced by this contributor must be accounted in the budget. This contributor is defined by both the polarisation sensitivity of the instrument and the degree of polarisation (DoP) of the incoming signal.

  The first of these has been calculated as the linear combination of the sensitivity of the filters, splitter and telescope to polarization (worst case). The results provided values lower than a 1% for the VNIR channels (except B1 with a 1.2%) and around 1.7% for the SWIR channels:

  The DoP of the incoming signal has not been assessed so far. The resulting uncertainty is, thus, the product of the polarisation sensitivity of the instrument and the DoP of the signal. Although the polarisation sensitivity of the MSI is very low, the final impact on the L1-C radiometry (and higher level products) will depend on the polarisation of the upcoming TOA radiance.

3.3. Uncertainty Contributors: A(b)

The correspondence between the instrument numerical count and the input radiance is determined by the absolute calibration coefficients. A mathematical model describing these coefficients is presented below:

$$A(b) = \frac{1}{N_p \cdot N_l \cdot N_d} \cdot \sum_{p,l,d} \frac{\pi \cdot Y_{sd}(p,l,b,d) \cdot d_{sun}^2}{K_{slt} \cdot \rho(p,\theta_{sd}(l),\phi_{sd}(l)) \cdot E_{sun}(b) \cdot \cos\theta_{sd}(l)} \quad (3)$$

where the term $Y_{sd}(p,l,b,d)$ refers to the dark signal corrected signal measured in calibration mode. The term $N_p \cdot N_l \cdot N_d$ is the product of the number of samples per pixel, line and detector collected during the calibration measurement. The satellite-to-sun distance (d_{sun}^2) can be well determined and it is not expected to be a source of uncertainty.

The main sources of uncertainty have been identified as:

- *Solar diffuser uncertainty:* this contribution is directly related to the reflectance term $\rho(p,\theta_{sd}(l),\phi_{sd}(l))$. It has been assessed by four main contributions: the bidirectional reflectance distribution function (BRDF) calibration, the diffuser polarisation, the diffuser non-uniformity and the observation angle.

  The first one of these has been obtained by combining quadratically the BRDF calibration uncertainty sources provided by the supplier.The diffuser polarisation has been calculated by multiplying the MSI polarisation sensitivity by the diffuser polarisation which has been estimated at 4% as a worst case. The values were lower than 0.1% for all the bands

  The diffuser non-uniformity uncertainty has been set to 1% specified as the requirement for the instrument. The observation angle uncertainty has been set to an initial value of 0.3%.

- *Straylight in calibration mode:* its effect has been estimated at around 0.7% by the instrument prime-contractor. However, a correction for this uncertainty contribution has been introduced in the mathematical model (referred as the coefficient K_{slt} in (3)). Thus, only its random residual effect will be accounted in the budget.

- *MSI noise in calibration mode:* this noise is the combination of the dark noise, readout noise, electronic noise and shot noise. As the noise is proportional to the input signal, the uncertainty for this contribution has been provided as a percentage of the incoming radiance. The noise measurements were calculated at L_{ref} and equation (2) was used to translate those values at L_{cal} (where L_{cal} refers to the estimated level of radiance measured during the sun-diffuser calibration). This signal is calculated as an average of the samples over a 10.8 acquisition of the sun-diffuser. Thus, the resulting uncertainty has been calculated as the experimental standard deviation of the mean (see [5]).

- *Angular knowledge-effect BRDF:* this contribution accounts for the shutter positioning and micro-vibrations that influence the knowledge of the angular position and, thus the term $\rho(p,\theta_{sd}(l),\phi_{sd}(l))$

- *Angular knowledge-effect incident beam:* this term accounts for the lack of knowledge in the incidence

angle. It is translated into an uncertainty on the cosine response of the diffuser (referred as $\cos\theta_{sd}(l)$ in (3)).

- *Ageing effect*: it accounts for the degradation in the performance of the diffuser. This uncertainty has been set to 1% based on previous experience as for example the diffusers on board of the MEdium Resolution Imaging Spectrometer (MERIS)[9]. However, this allocation could be highly reduced since it is known that the organic contamination is the cause of the ageing of the diffuser material and it has been minimized during the manufacture of the S2 diffusers [10]

- *DS error during calibration:* this refers to the random component after the subtraction of the DS during the ground processing (see Fig.1b). This effect will be reduced by averaging the samples acquired during the calibration measurement.

- *Sun irradiance:* its effect is cancelled out when the reflectance is calculated. However, an assessment of its impact on the radiance uncertainty budget is necessary.

  The level of uncertainty is associated with the term $E_{sun}(b)$, which refers to the sun irradiance value for each band based on the Thuillier model [8]. We have identified three main sources of uncertainty for this contributor: the propagation of the band spectral uncertainty, and the model uncertainty.

  The first of the contributions has been assessed by propagating the bandwidth and central wavelength uncertainty values. And the second contribution has been assessed by comparing the irradiance levels for the Sentinel-2 bands using the Thuillier model [8] and the Kurucz model [11].

3.4. Uncertainty Contributors: DS(p,l,mod6,d) & PCmasked(l,b,d)

The DS is determined by processing images with the lowest possible incoming radiance. Image acquisition takes place at night over the ocean with the MSI CSM (Calibration and Shutter Mechanism) opened. The dark signal measurement takes at least 10.8 seconds in order to average the noise. The decompressed signal $X(p,l,b,d)$ is averaged over the lines modulo 6 for 10 m bands, modulo 3 for 20 m bands and over all lines for 60 m bands. The equation describing this process is given below (N is the number of lines being summed):

$$DS(p,l \bmod i,b,d) = \frac{\sum_{l \bmod i} X(p,l,b,d)}{N_{l \bmod i}} \quad (4)$$

The term *MSI temporal & compression noise* accounts for the standard deviation of the mean from the samples acquired during the dark signal measurement. The compression noise in this case is negligible.

The term *Dark signal stability* takes into account the fluctuation of the DS value between two measurements taken every two weeks. During the commissioning phase this evolution will be monitored and an uncertainty for this contributor will be given and/or a correction applied.

3.5. Uncertainty Contributors: γ(p,l,b,Y)

The absolute calibration coefficient (A(b)) is measured for a specific level of radiance (L_{cal}). However, those coefficients are used for the whole dynamic range. The γ-function compensates for the non-linear response over the dynamic range and corrects for non-uniform response of the pixels.

The γ-function is characterised on-ground for every pixel. However, each pixel will evolve with time in a different way. Therefore, the difference in the relative evolution of each pixel to the overall channel (measured by the absolute calibration coefficient) must be studied. The response of the γ-function is updated in-flight and Equation 5a models this procedure:

$$\gamma_{updated}(p,b,d,Y) = \gamma_{ground}\left(p,b,d,\frac{\gamma_{ground}^{-1}\left(p,b,d,\overline{Z_{sd}(p,b,d)}\right)}{Y_{sd}(p,b,d)}\cdot Y\right) \quad (5a)$$

where $Z_{sd}(p,b,d)$ is the theoretical equalized signal described as:

$$\overline{Z_{sd}(p,b,d)} = A(b)\cdot K_{slt}\cdot\frac{1}{N_l}\cdot \sum_l \frac{\rho(p,\theta_{sd}(l),\phi(l))}{\pi}\cdot\frac{E_{sun}(b)}{d_{sun}^2}\cdot\cos\theta_{sd}(l) \quad (5b)$$

and the term $\overline{Y_{sd}(p,b,d)}$ accounts for the averaged signal obtained during the measurement (taken in calibration mode) and modeled as:

$$\overline{Y_{sd}(p,b,d)} = \frac{1}{N_l}\cdot\sum_l Y_{sd}(p,l,b,d) \quad (5c)$$

The S2 linearity requirement has been set to 1%. The resulting level of uncertainty will be the residual after

applying the γ-function. As an initial value it has been set to a conservative value 0.4%. However, a precise uncertainty assessment of this parameter may result in a lower uncertainty level.

3.6. Summation

The equation below proposes a quadratic summation to combine the previous uncertainty parameters:

$$u^2_{R_{L1c}(p,b)} = u^2_{\gamma(p,b,d,\ \gamma p,l,b,d))} + u^2_{X(p,l,b,d)} + u^2_{DS(p,l\mathrm{modi},d)} + \\ + u^2_{A(b)} + u^2_{denoising} + u^2_{resampling} + R_{L1c}(p,b)^2 * \mathrm{cov} \quad (6)$$

where u_j means the uncertainty at 1-sigma of the contributor j in % units and the 'cov' term refers to the covariance matrix with values ranging from 0 to 1. In this report its effect has not been studied. The assumption of uncorrelated contributors is unrealistic and, therefore, its effect should be studied in future.

This summation is only valid when all signed biases have been corrected (see GUM [5]). This is the case of *straylight in calibration* where a correction has been applied and introduced as part of the model (see Equation 3). However, there are two other signed bias effects, the *straylight in nominal mode* and the *ageing effect*, that have not been corrected so far.

The first one of them is expected to be measured and quantified on-ground and a subsequent correction coefficient will be introduced to compensate for such effect (similarly to the *straylight in calibration*) whereas the second one will be more difficult to estimate. As shown in [9], the *ageing effect* was monitored in the MERIS instrument comparing to a second diffuser on-board. The S2 does not include a second diffuser and an in-flight estimation becomes more complicated. Alternative methods should be developed to account for this bias.

4. SENTINEL-2 RADIOMETRIC UNCERTAINTY TOOL (S2-RUT)

The main objective of the S2-RUT tool is the determination, from a Sentinel-2 Level-1C product (TOA reflectance/radiance image), the absolute radiometric uncertainty of each measurement pixel as recommended in the QA4EO guidelines [6].

The radiometric model, uncertainty contributors and their combination have been implemented in a software package that includes the source code and the binaries as well as full documentation of the tool.

In this chapter we briefly describe the S2-RUT source code schematic (section A) and the inputs and outputs of the tool (section B).

4.1. S2-RUT flow schematic

Fig.2 presents a flow diagram of the S2-RUT. The blue lines indicate inputs, the dashed black lines refer to the call of function of a module from another module and the red lines indicate the outputs.

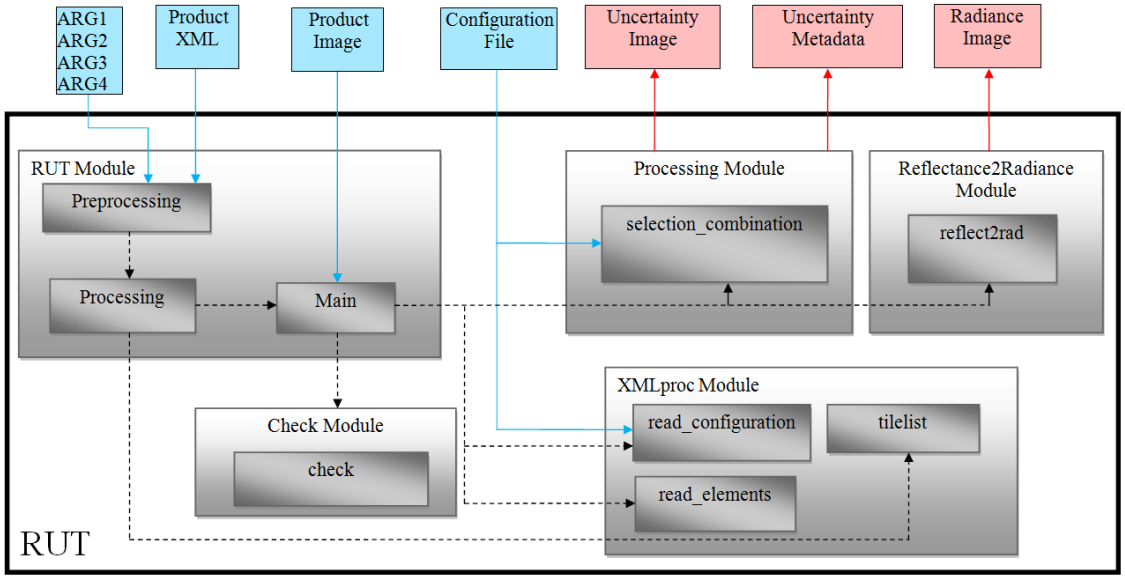

Figure 2. S2-RUT flow diagram. The blue lines indicate inputs, the dashed black lines refer to the call of function of a module from another module and the red lines indicate the outputs.

In the ‘main’ routine the S2 L1-C image is read and the pixel values are saved as an array. Following this, the ‘read elements’ and ‘read_configuration’ routines are called in order to read the product metadata and the configuration file. These two provide all the necessary parameters in order to calculate the uncertainty and the radiance conversion. Then, a module named ‘check.py’ executes specific processing depending on the parameters and/or flags in the product metadata (e.g. crosstalk uncertainty will not be accounted for if there is a flag indicating that a correction has been applied).

In a next step the ‘reflect2rad’ module is executed. It converts the reflectance into radiance values. This resulting radiance image is coded in JPEG-2000 format and provided as an output.

Finally, in ‘selection_combination’ the major calculations are done. First an interpolation of the radiance range values is generated and the level of uncertainty for each contributor is selected depending on the pixel radiance. These contributors are combined to get a 1-sigma uncertainty value for each pixel. Finally, the uncertainty values are converted into a JPEG-2000 image and basic information is provided in a metadata output file.

4.2. Inputs and outputs

In Fig.3, we show an example of a S2 L1-C reflectance image, the resulting radiance image and the associated reflectance uncertainty image. The reflectance image corresponds to a S2 simulated product of the band 9. In addition, it is possible to appreciate the inverse relationship between the reflectance pixels and their corresponding uncertainty pixels. This is because the uncertainty associated to each pixel is based on its specific reflectance value

.

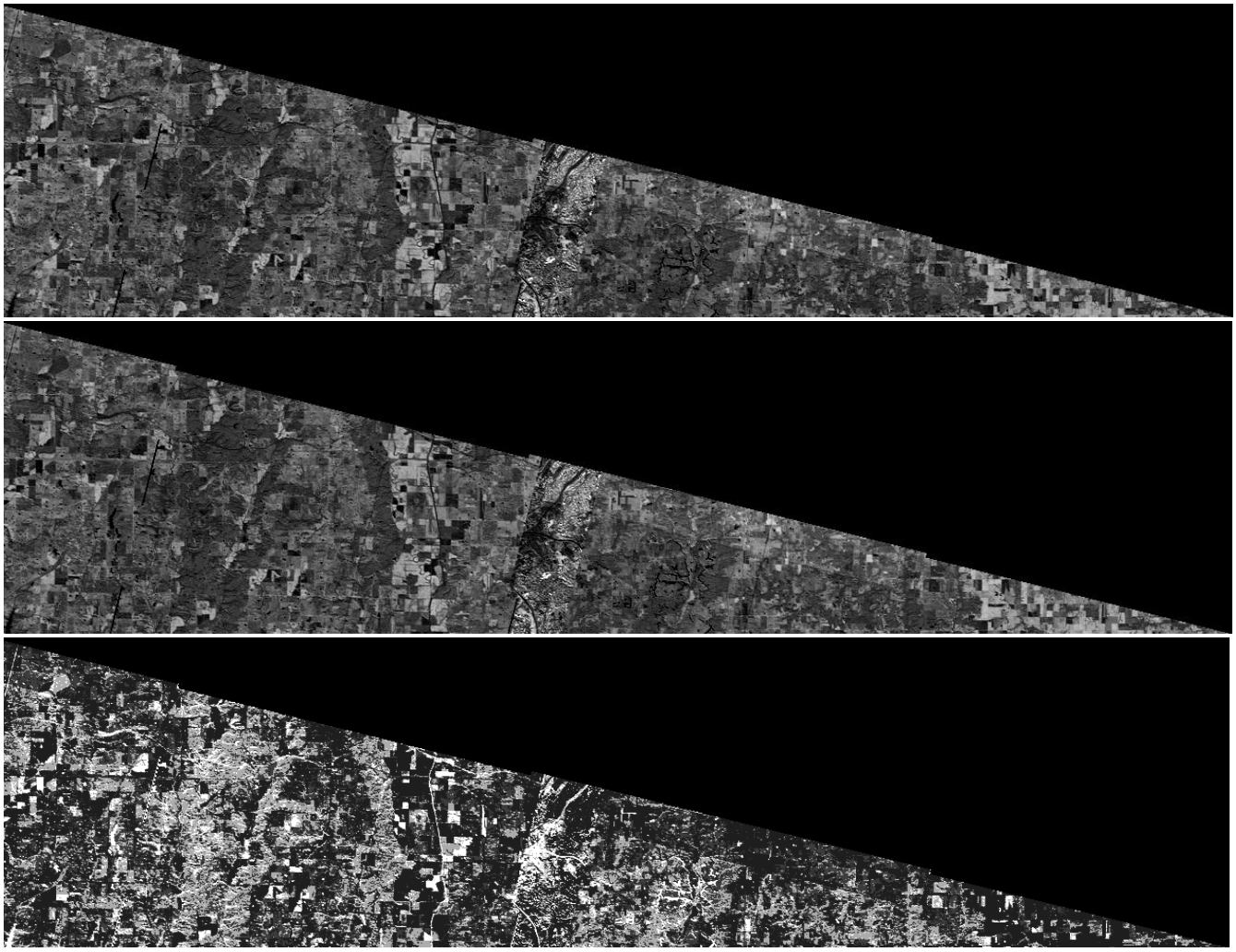

Figure 3. (Top) S2 L1-C Reflectance image of band 9 from a simulated product and the resultant (centre) radiance image and (bottom) reflectance uncertainty image

The tool can work in two different modes: 'Reflectance' or 'Radiance' (ARG2 in Fig.2). If 'Reflectance' is selected, a JPEG-2000 image with the reflectance uncertainty will be given as output, together with a metadata file containing basic information such as the mean uncertainty, maximum and minimum uncertainty, etc.

If 'Radiance' is selected, then a JPEG-2000 image with the radiance uncertainty and an associated metadata file will be generated in a similar manner to the previous case, but the S2 L1-C product reflectance image will be converted into a JPEG-2000 radiance image and it will be given as an output as well (see Fig. 3).

Apart from the Reflectance/Radiance selection, the S2 L1-C product is needed as an input. The main product data consists of a JPEG-2000 reflectance image for each band and an associated metadata file [4]. The specific product to be processed will be indicated by providing the directory (ARG1 in Fig.2) where it is located. There is, in addition, the possibility to specify a concrete band and tile (ARG3 and ARG4 in Fig.2) from the product.

5. CONCLUSIONS & FURTHER WORK

A first prototype version of the S2-RUT for the future Sentinel-2 satellite mission has been presented. The final objective of the project is to provide the user with a radiometric uncertainty per pixel based in a transparent and traceable radiometric uncertainty analysis outlined in the QA4EO guidelines [6]. Where possible, an assessment of the uncertainty contributor and/or correction is given and, where not, potential methods are indicated.

This first approach is expected to be improved by future reviews pre-launch and during the mission life-time. Throughout this paper, different approaches to improve the tool have been suggested. Specifically, our main suggestion for future versions is an in-depth study of the uncertainty dependence on the position in the field of view for each individual detector and band. In order to obtain such information the tool will need to undo the resampling present in the S2-L1C product or propagate those uncertainties to the resampled image.

REFERENCES

1. Schulte-Braucks, R. (2013). Observing the Land Beyond. *International Innovation*. Online at *http://copernicus.eu/fileadmin/user_upload/Docs_for_Pages/Article_International_innovation_RSB_April_2013.pdf*

2. Aschbacher, J. (2012). GMES Space Component getting ready for operations. *European Space Agency*, Bulletin 149. Online at *http://esamultimedia.esa.int/docs/EarthObservation/Bullletin149_GMES.pdf*

3. European Space Agency (2010). GMES Sentinel-2 mission requirements document. Issue 2 revision 1. Online at *http://esamultimedia.esa.int/docs/GMES/Sentinel-2_MRD.pdf*

4. Drusch, M. et al. (2012). Sentinel-2: ESA's Optical High-Resolution Mission for GMES Operational Services. Remote Sensing of Environment, 120, 25-36.

5. JCGM 100:2008 (2008). Evaluation of measurement data - Guide to the expression of uncertainty in measurement (GUM). *Joint Committee for Guides in Metrology*. Online at *http://www.bipm.org/utils/common/documents/jcgm/JCGM_100_2008_E.pdf*

6. QA4EO task team (2010). A Quality Assurance Framework for Earth Observation: Principles. *QA4EO*, Version 4.0. Online at *http://www.qa4eo.org/docs/QA4EO_Principles_v4.0.pdf*

7. Fox, N. (2010). A guide to expression of uncertainty of measurements. *QA4EO*, Version 4.0. Online at *http://www.qa4eo.org/docs/QA4EO-QAEO-GEN-DQK-006_v4.0.pdf*

8. Thuillier, G. et. al. (2013). The Solar Spectral Irradiance from 200 to 2400 nm as Measured by the SOLSPEC Spectrometer from the ATLAS and EURECA Missions. *Solar Physics*, 214, 1–22.

9. Jackson, J. (2008). MERIS 65th cyclic report 7th January 2008 - 11th February 2008. *European Space Agency*, MERIS cyclic report. Online at *http://earth.eo.esa.int/pcs/envisat/meris/reports/cyclic/MERIS_CR_065_080107_080211.pdf*

10. Leland, J. E. and Arecchi, A. V. (1995). Phase 2 analysis of Spectralon material for use in on-board calibration systems for the medium-resolution imaging spectrometer (MERIS). *Proc. SPIE, Infrared Detectors and Instrumentation for Astronomy*, 2475(384).

11. Chance, K. and Kurucz, R.L. (2010). An improved high-resolution solar reference spectrum for Earth's atmosphere measurements in the ultraviolet, visible, and near infrared. *Journal of Quantitative Spectroscopy & Radiative Transfer*, 111, 1289–1295.